

Support Information

Achieving High Activity and Long-Term Stability towards Oxygen Evolution in Acid by Phases Coupling between CeO₂-Ir



Figure S1. The pH of 0.5 M H₂SO₄ at room temperature.

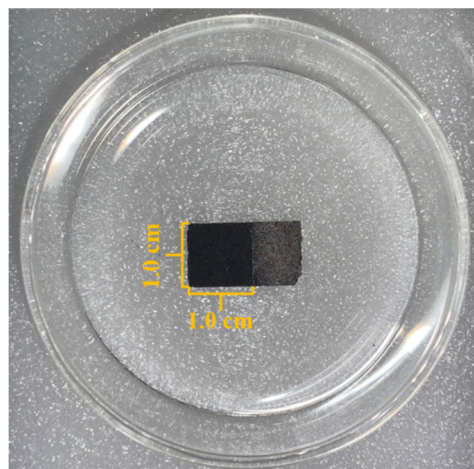


Figure S2. Photograph of catalyst-loaded carbon paper.

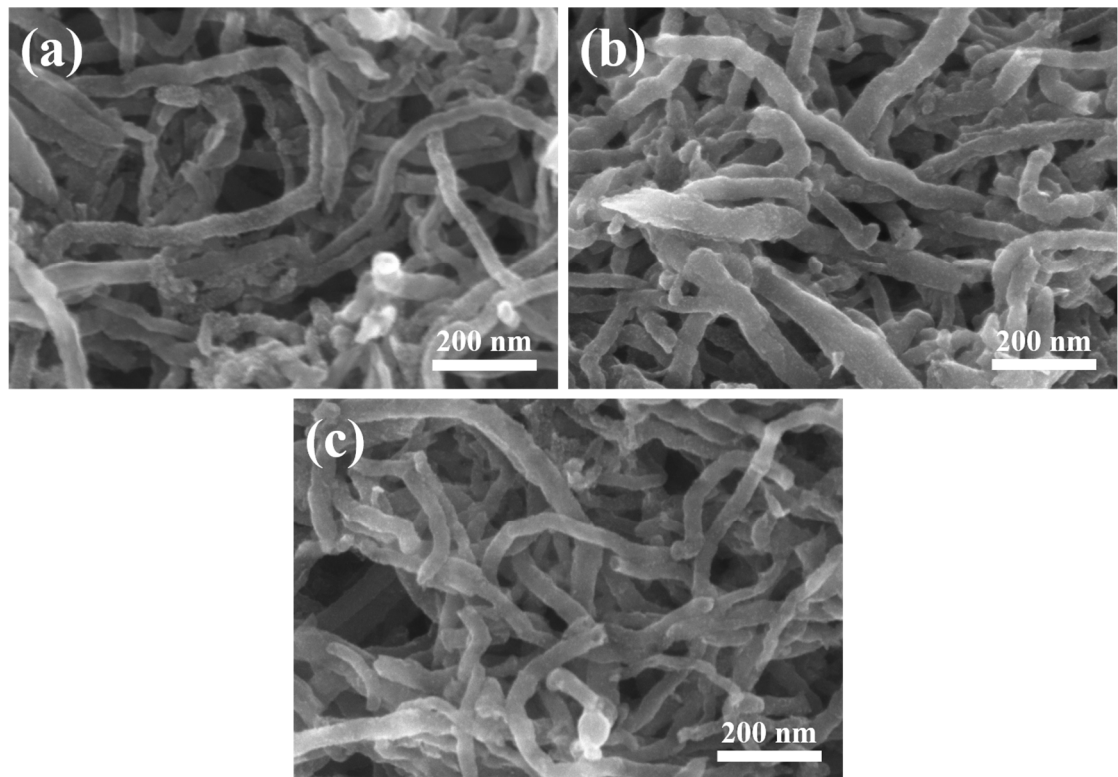


Figure S3. SEM images of (a) CeO₂-Ir/CNTs, (b) Ir/CNTs and (c) CeO₂/CNTs.

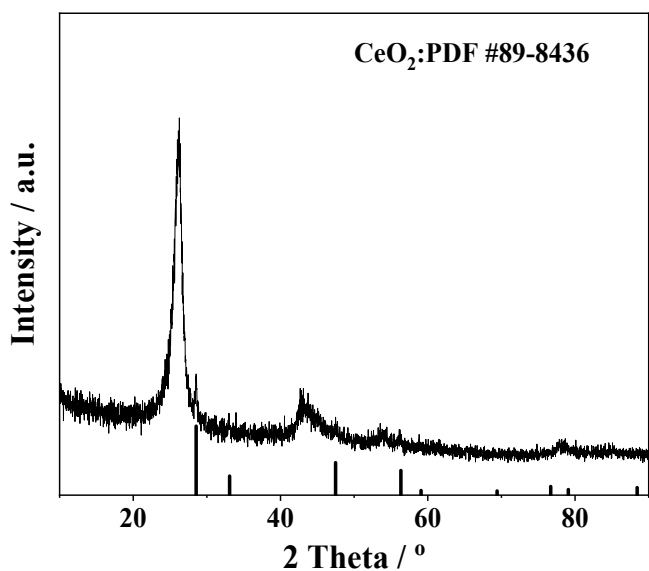


Figure S4. XRD pattern of CeO₂/CNTs.

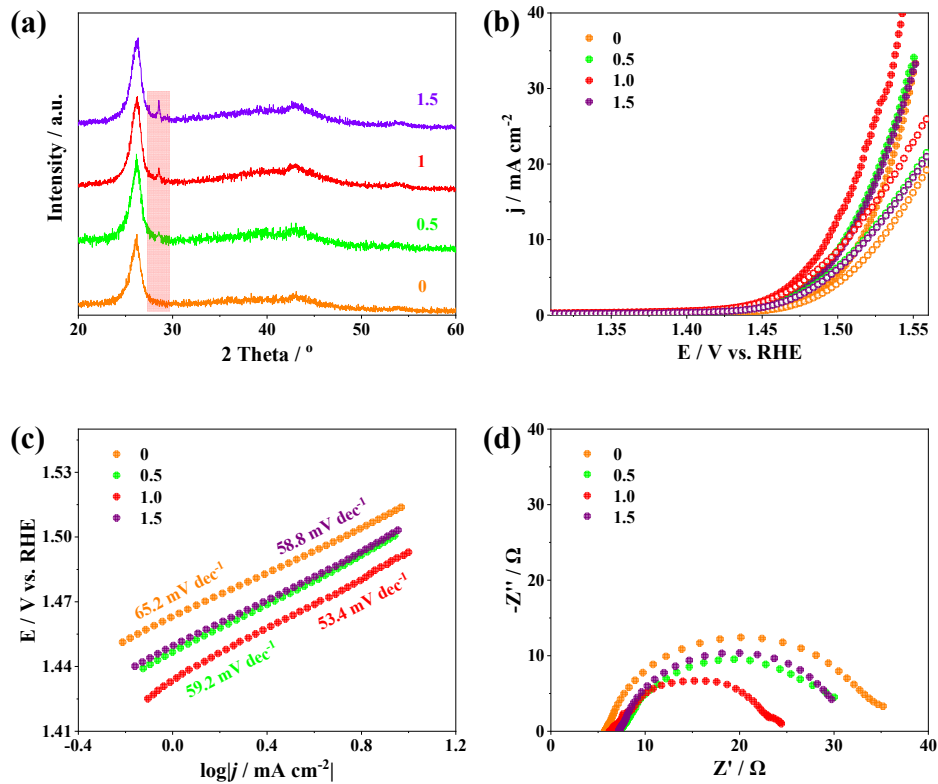


Figure S5. (a) XRD patterns, (b) LSVs (solid-dot line: with iR compensation), (c) Tafel plots and (d) EIS Nyquist plots of $x\text{CeO}_2\text{-Ir/CNTs}$ with different CeO_2 content.

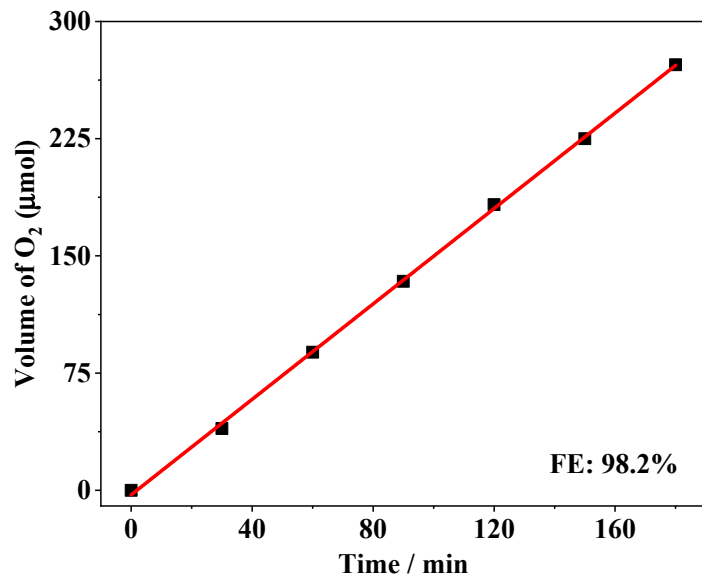


Figure S6. The time-dependent volume of O_2 towards OER using $\text{CeO}_2\text{-Ir/CNTs}$ as anode. The red line represents a fitted line, while square data points denote the volume of O_2 generated at 30-minute intervals.

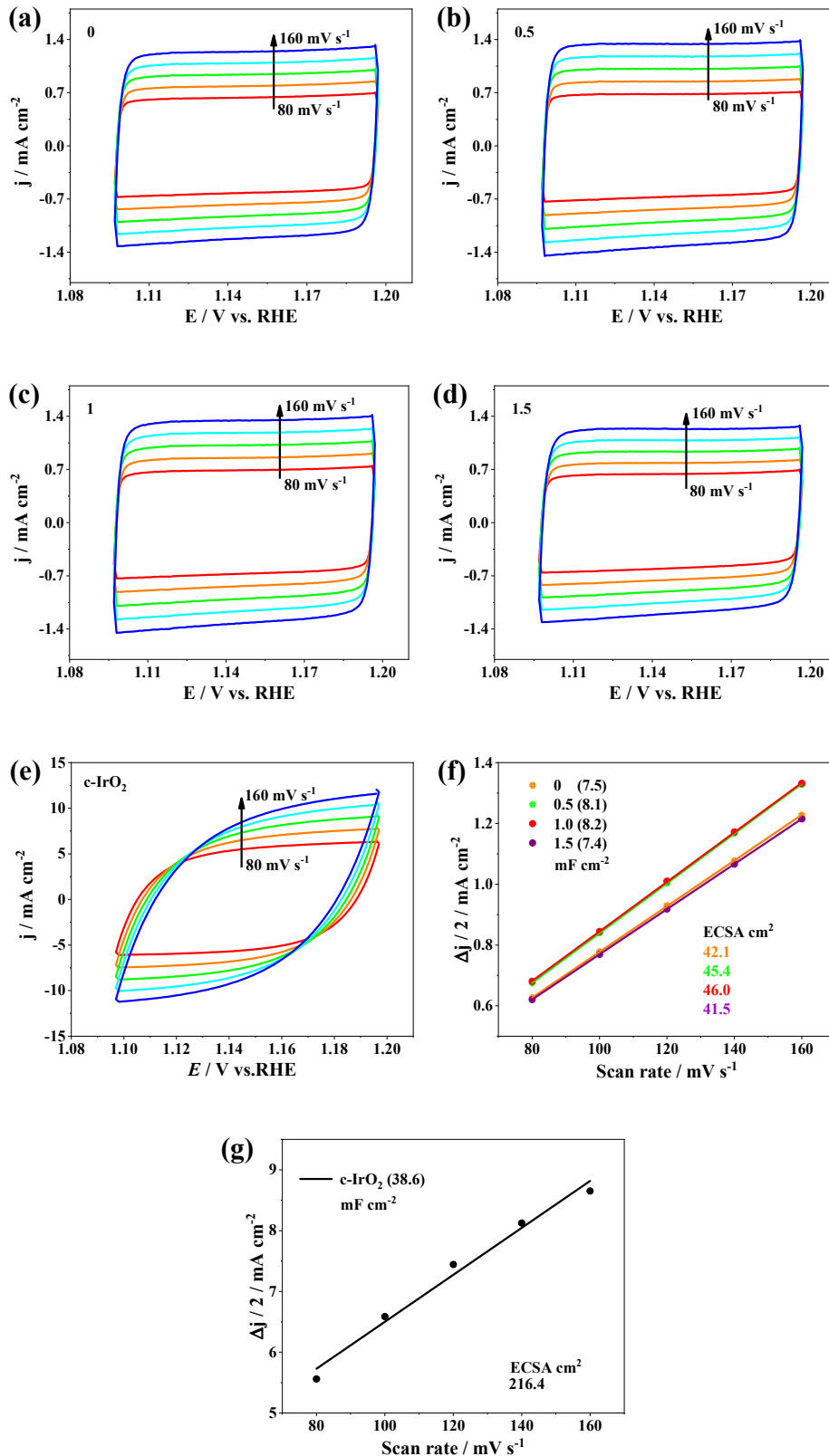


Figure S7. CVs recorded at different scan rates in the region of 1.1-1.2 V of (a-d) xCeO₂-Ir/CNTs with different CeO₂ content and (e) c-IrO₂. (f) and (g) C_{dl} plots and ECSAs of the catalysts.

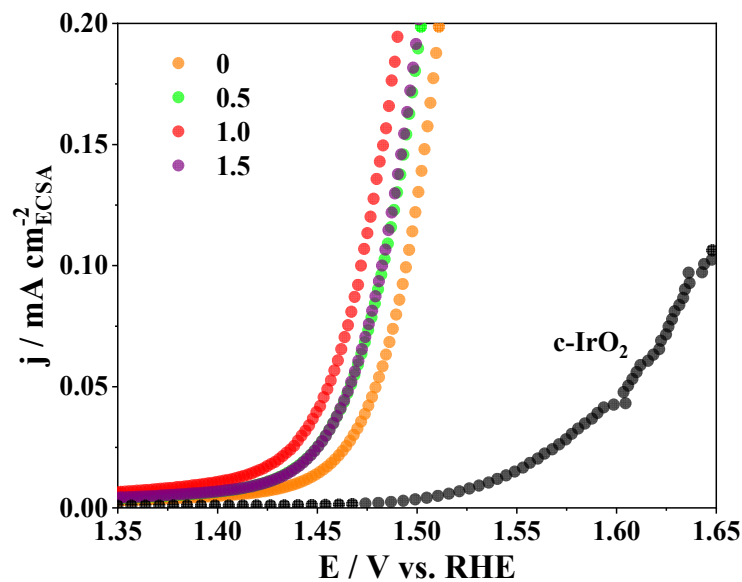


Figure S8. ECSA-normalized LSVs of $x\text{CeO}_2\text{-Ir/CNTs}$ and c-IrO_2 .

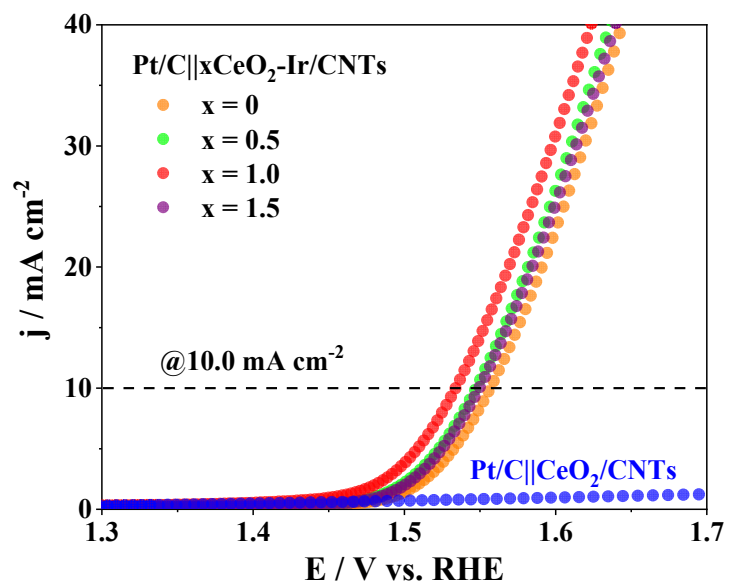


Figure S9. LSVs of $\text{Pt/C}||x\text{CeO}_2\text{-Ir/CNTs}$ and $\text{Pt/C}||\text{CeO}_2\text{/CNTs}$.

Table S1. Composition analysis of xCeO₂-Ir/CNTs.

xCeO ₂ -Ir/CNTs	Mass Concentration / mg L ⁻¹		Atomic Concentration / mmol L ⁻¹		Atomic ratio Ce:Ir
	Ce	Ir	Ce	Ir	
x = 0	0	56.161	0	0.292	0
x = 0.5	20.635	56.772	0.147	0.295	0.498
x = 1	41.327	56.568	0.295	0.294	1.003
x = 1.5	62.006	56.572	0.443	0.294	1.507

Table S2. Analysis of EDS spectrum.

Element	Atomic Fraction (%)	Mass Fraction (%)
C	94.70	84.94
O	4.52	5.41
Ce	0.39	4.07
Ir	0.39	5.58

Table S3. OER performance comparison of the CeO₂-Ir/CNTs with the catalysts reported in acid media.

Catalyst	Electrolyte	Mass loading	η_{10} (mV)	Stability (h @ η_{10})	Mass activity (A g ⁻¹ @V)	Ref.
CeO ₂ -Ir/CNTs	0.5 M H ₂ SO ₄	~0.20 mg cm ⁻²	262.9	60	2542.3 @1.53	This work
Li-IrO _x	0.5 M H ₂ SO ₄	0.125 mg cm ⁻²	290	10	100 @1.52	[1]
IrO ₂ @Ir/TiN	0.5 M H ₂ SO ₄	0.379 mg·cm ⁻²	265	6	480.4 @1.6	[2]
Ir@N-G-750	0.5 M H ₂ SO ₄	23 $\mu\text{g}\cdot\text{cm}^{-2}$	303	20*	2420 @1.6	[3]
IrGa/N-rGO	0.5 M H ₂ SO ₄	-	275	-	-	[4]
Sr ₂ IrO ₄	0.5 M H ₂ SO ₄	0.404 mg cm ⁻²	263			[5]
IrO ₂ /V ₂ O ₅	0.5 M H ₂ SO ₄	0.1 mg _{Ir} cm ⁻²	266	20	287 @1.53	[6]
IrCo NRAs	0.5 M H ₂ SO ₄	-	296.9	15	315.5 @1.51	[7]
Ru@IrO _x	0.5 M H ₂ SO ₄	~0.051 mg _{oxide} cm ⁻²	282	24	644.8 @1.56	[8]
Ir-CeO ₂ -C	0.5 M H ₂ SO ₄	1 mg cm ⁻²	283	60	21.95 @1.53	[9]
IrO _x /SrIrO ₃	0.5 M H ₂ SO ₄	-	~270	30	-	[10]
IrMoO _x	0.5 M H ₂ SO ₄	0.816 mg _{oxide} cm ⁻²	267	30	-	[11]
IrNiO _x	0.5 M H ₂ SO ₄	10.2 $\mu\text{g}_{\text{Ir}} \text{cm}^{-2}$	~309	-	170 @1.50	[12]
Ir ₆ Ag ₉ NTs/C	0.5 M H ₂ SO ₄	13.3 $\mu\text{g}_{\text{Ir}} \text{cm}^{-2}$	285	6	-	[13]
La ₂ LiIrO ₆	0.5 M H ₂ SO ₄	0.255 mg _{oxide} cm ⁻²	278	-	-	[14]

*denotes the OER durability tested in 0.1 M HClO₄.

Table S4. Component analysis of CeO₂-Ir/CNTs before and after OER.

CeO ₂ -Ir/CNTs				
	Before OER		Post OER	
Element	Ce	Ir	Ce	Ir
Mass concentration / mg L ⁻¹	41.327	56.568	29.479	54.742
Atomic Concentration / mmol L ⁻¹	0.295	0.294	0.210	0.285
Atomic ratio	Ce:Ir = 1.003		Ce:Ir = 0.737	

References

- Gao, J.; Xu, C.-Q.; Hung, S.-F.; Liu, W.; Cai, W.; Zeng, Z.; Jia, C.; Chen, H. M.; Xiao, H.; Li, J.; Huang, Y.; Liu, B., Breaking long-range order in iridium oxide by alkali ion for efficient water oxidation. *J. Am. Chem. Soc.* **2019**, 141, 3014-3023.
- Li, G.; Li, K.; Yang, L.; Chang, J.; Ma, R.; Wu, Z.; Ge, J.; Liu, C.; Xing, W., Boosted performance of Ir species by employing TiN as the support toward oxygen evolution reaction. *ACS Appl. Mater. Interfaces* **2018**, 10, 38117-38124.
- Wu, X.; Feng, B.; Li, W.; Niu, Y.; Yu, Y.; Lu, S.; Zhong, C.; Liu, P.; Tian, Z.; Chen, L.; Hu, W.; Li, C. M., Metal-support interaction boosted electrocatalysis of ultrasmall iridium nanoparticles supported on nitrogen doped graphene for highly efficient water electrolysis in acidic and alkaline media. *Nano Energy* **2019**, 62, 117-126.
- Zhang, H.; Shi, P.; Ma, X.; Ma, C.; Han, S.; He, C.; Wu, H.; Zhu, L.; Zhang, B.; Lu, Y.; Cao, W.; Yin, H.; Meng, X.; Xia, J.; Zhang, J.; Wang, A.-L.; Lu, Q., Construction of ordered atomic donor-acceptor architectures in bcc IrGa intermetallic compounds toward highly electroactive and stable overall water splitting. *Adv. Energy Mater.* **2022**, 13, 2202703.
- Zhang, L.; Jang, H.; Li, Z.; Liu, H.; Kim, M. G.; Liu, X.; Cho, J., SrIrO₃ modified with laminar Sr₂IrO₄ as a robust bifunctional electrocatalyst for overall water splitting in acidic media. *Chem. Eng. J.* **2021**, 419, 129604.
- Zheng, X.; Qin, M.; Ma, S.; Chen, Y.; Ning, H.; Yang, R.; Mao, S.; Wang, Y., Strong oxide-support interaction over IrO₂/V₂O₅ for efficient pH-universal water splitting. *Adv. Sci.* **2022**, 9, 2104636.
- Zhang, Y.; Zhang, G.; Zhang, M.; Zhu, X.; Shi, P.; Wang, S.; Wang, A.-L., Synergistic electronic and morphological modulation by trace Ir introduction boosting oxygen evolution performance over a wide pH range. *Chem. Eng. J.* **2022**, 433, 133577.
- Shan, J.; Guo, C.; Zhu, Y.; Chen, S.; Song, L.; Jaroniec, M.; Zheng, Y.; Qiao, S.-Z., Charge-redistribution-enhanced nanocrystalline Ru@IrO_x electrocatalysts for oxygen evolution in acidic media. *Chem* **2019**, 5, 445-459.
- Chen, X.; Liao, W.; Zhong, M.; Chen, J.; Yan, S.; Li, W.; Wang, C.; Chen, W.; Lu, X., Rational

- design of robust iridium-ceria oxide-carbon nanofibers to boost oxygen evolution reaction in both alkaline and acidic media. *Nano Res.* **2022**, 16, 7724-7732.
- 10. Seitz, L. C.; Dickens, C. F.; Nishio, K.; Hikita, Y.; Montoya, J.; Doyle, A.; Kirk, C.; Vojvodic, A.; Hwang, H. Y.; Norskov, J. K.; Jaramillo, T. F., A highly active and stable $\text{IrO}_x/\text{SrIrO}_3$ catalyst for the oxygen evolution reaction. *Science* **2016**, 353, 1011-1014.
 - 11. Chen, X.; Li, W.; Song, N.; Zhong, M.; Yan, S.; Xu, J.; Zhu, W.; Wang, C.; Lu, X., Electronic modulation of iridium-molybdenum oxides with a low crystallinity for high-efficiency acidic oxygen evolution reaction. *Chem. Eng. J.* **2022**, 440, 135851.
 - 12. Nong, H. N.; Reier, T.; Oh, H.-S.; Gliech, M.; Paciok, P.; Vu, T. H. T.; Teschner, D.; Heggen, M.; Petkov, V.; Schlögl, R.; Jones, T.; Strasser, P., A unique oxygen ligand environment facilitates water oxidation in hole-doped IrNiO_x core–shell electrocatalysts. *Nat. Catal.* **2018**, 1, 841-851.
 - 13. Zhu, M.; Shao, Q.; Qian, Y.; Huang, X., Superior overall water splitting electrocatalysis in acidic conditions enabled by bimetallic Ir-Ag nanotubes. *Nano Energy* **2019**, 56, 330-337.
 - 14. Grimaud, A.; Demortiere, A.; Saubanere, M.; Dachraoui, W.; Duchamp, M.; Doublet, M.-L.; Tarascon, J.-M., Activation of surface oxygen sites on an iridium-based model catalyst for the oxygen evolution reaction. *Nat. Energy* **2016**, 2, 16189.